Parameter Name	ICC (Low 95%CI-High 95%CI)
BMO Area	0.55 (0.06-0.91)
BMO Radius	0.54 (0.05-0.90)
BMO Depth	0.97 (0.87-0.99)
ASCO Area	0.93 (0.77-0.99)
ASCO Radius	0.93 (0.77-0.99)
ASCO Depth	0.81 (0.45-0.96)
ASCO H/V	0.76 (0.36-0.96)
PSCO Area	0.75 (0.34-0.95)
PSCO Radius	0.77 (0.38-0.96)
PSCO Depth	0.58 (0.10-0.91)
PSCO H/V	0.85 (0.54-0.97)
ON-ASCO Area	0.95 (0.84-0.99)
ON-ASCO Radius	0.95 (0.83-0.99)
ON-ASCO H/V	0.85 (0.55-0.97)
ON-PSCO Area	0.98 (0.91-0.99)
ON-PSCO Radius	0.98 (0.91-0.99)
ON-PSCO H/V	0.97 (0.87-0.99)
ON-Volume	0.88 (0.62-0.98)
ASCO-ON-ASCO distance	0.93 (0.75 -0.99)
PSCO-ON-PSCO distance	0.49 (0 - 0.89)
Scleral thickness	0.71 (0.28-0.95)
Scleral Depth	0.95 (0.82-0.99)
Choroidal Thickness	0.55 (0.06-0.91)

ICC - Intraclass Correlation Coefficient , **CI**- Confidence Interval
ICC grading: <0.4 - Poor Reproducibility; 0.4-0.75-Fair to Good Reproducibility; >0.75-Excellent Reproducibility. Only parameters with Fair to Good or excellent reproducibility were included in this report.

Supplemental Table 1 - Reproducibility Data

Parameter[1]	Rat Number															
	Rat 1		Rat 2		Rat 3		Rat 4		Rat 5		Rat 6[2]		Rat 7		Rat 8	
	C	EG	C	EG	C	EG	C	EG	C	EG	C	EG	C	EG	C	EG
NeurovascularCanal																
BMO Area (μm^2)	$6.15x10^4$	$5.88 x10^4$	$4.76 x10^4$	$5.69 x10^4$	$5.26x10^4$	$5.45 x10^4$	$5.71 x10^4$	$6.11 x10^4$	$5.18 x10^4$	$5.86 x10^4$	$6.90 x10^4$	$6.72 x10^4$	$5.40 x10^4$	$6.50x10^4$	$5.83x10^4$	$6.84x10^4$
BMO Radius (µm)	139±18	135±19	122±14	**133±22***	129±11	131±9	135±6	**139±10***	128±12	**136±13***	148±8	146±8	131±10	**144±9***	136±7	**147±10***
BMO Depth	16±11	**38±11***	47 ±9	**26±7***	39±5	**51±10***	36±9	34±6	26±10	**28±9***	37±6	**56±6***	-1±5	**27±9***	33±8	**22±6***
ASCO Area (μm^2)	$1.49x10^5$	$1.45 x10^5$	$1.22x10^5$	$1.45 x10^5$	$1.23x10^5$	$1.60 x10^5$	$1.02 x10^5$	$1.50 x10^5$	$1.57 x10^5$	$2.09 x10^5$	$1.06 x10^5$	$150 x10^5$	$1.38 x10^5$	$1.69 x10^5$	$1.33 x10^5$	$1.55 x10^5$
ASCO Radius (µm)	216±25	213±31	196±21	**215±10***	196±29	**225±21***	180±16	**217±21***	223±16	**256±33***	183±18	**217±22***	209±16	**231±26***	205±25	**221±24***
ASCO H/V Ratio	1.24	1.37	1.26	1.01	1.42	1.28	1.26	1.19	1.11	1.24	1.25	1.26	1.17	1.31	1.38	1.27
ASCO Depth	78±22	78 ±18	104±20	**74±19***	112 ±18	117±17	105 ±16	**87±22***	88 ±17	**104±20***	106±23	106±12	73±13	77±15	94±15	91±9
PSCO Area (μm^2)	$1.59x10^5$	$1.52 x10^5$	$1.13 x10^5$	$1.45 x10^5$	$1.40x10^5$	$1.72 x10^5$	$1.13 x10^5$	$1.47 x10^5$	$1.54x10^5$	$2.23 x10^5$	$1.22 x10^5$	NA	$1.58 x10^5$	$1.74 x10^5$	$1.09 x10^5$	$1.60 x10^5$
PSCO Radius (µm)	223 ±30	218±35	189 ±15	**214±16***	209 ±30	**233±21***	189 ±18	**215±26***	220±20	**263±42***	197±13	NA	223 ±17	**233±29***	185 ±23	**224±25***
PSCO H/V Ratio	1.47	1.15	1.10	1.06	1.40	1.21	1.20	1.23	1.13	1.38	1.21	NA	1.36	1.13	1.33	1.37
PSCO Depth	160±28	**153±22***	170±25	**142±27***	167±20	**181±25***	182 ±19	**163±27***	164 ±23	**182±36***	172±27	NA	141±23	**152±26***	171±29	**163±24***
Optic Nerve (ON)																
ON-ASCO Area (μm^2)	$4.54x10^4$	$5.66x10^4$	$4.26x10^4$	$4.13x10^4$	$4.36x10^4$	$6.88x10^4$	$4.46x10^4$	$5.90x10^4$	$5.37x10^4$	$6.45x10^4$	$4.73 x10^4$	$6.14 x10^4$	$4.16 x10^4$	$6.85 x10^4$	$5.20 x10^4$	$7.02 x10^6$
ON-ASCO Radius (µm)	117 ±27	**133±19***	112 ±33	112±26	114±32	**145±29***	115 ±32	**135±25***	128 ±29	**142±22***	120 ±28	**139±20***	112 ±25	**146±20***	127 ±24	**148±22***
ON-ASCO H/V Ratio	1.82	1.52	2.18	1.90	2.18	1.74	2.08	1.66	1.97	1.57	1.88	1.42	1.86	1.44	1.66	1.51
ON-PSCO Area (μm^2)	$4.81x10^4$	$4.99x10^4$	$4.28x10^4$	$4.78x10^4$	$4.14x10^4$	$6.79x10^4$	$3.99x10^4$	$5.61x10^4$	$5.34x10^4$	$6.39 x10^4$	$4.37 x10^4$	NA	$4.25 x10^4$	$6.52 x10^4$	$4.14 x10^4$	$7.44 x10^6$
ON-PSCO Radius (µm)	117 ±41	119±42	108±44	**117±39***	107±41	**142±39***	105±43	**128±40***	124±41	**139±31***	111±42	NA	112±33	**140±33***	106±43	**150±37***
ON-PSCO H/V Ratio	2.41	2.43	2.72	2.34	2.60	2.04	2.97	2.10	2.29	1.64	2.55	NA	1.89	2.18	1.81	2.75
ON Volume (μm^3)	$3.95x10^6$	$3.78x10^6$	$2.92x10^6$	$3.08x10^4$	$2.29x10^6$	$4.61x10^6$	$3.25x10^6$	$4.69x10^6$	$4.04x10^6$	$4.95 x10^6$	$3.20 x10^6$	NA	$2.88 x10^6$	$5.54 x10^6$	$3.67 x10^6$	$5.50 x10^6$
Optic Nerve to Scleral Canal Gap Distance																
ASCO-ON-ASCO Distance (µm)	91±48	80±24	84±20	**101±37***	82±19	78±26	64±22	**81±29***	94±31	**111±46***	63±20	**77±32***	95±26	**83±28***	76±28	73±19
PSCO-ON-PSCO Distance (µm)	104±41	98±20	81±34	**95±41***	101±31	**91±32***	83±42	87±22	96±38	**123±23***	86±35	NA	110±38	**92±29***	78±27	74±19
Sclera/Choroid																
Scleral Thickness (µm)	109±26	**101±17***	105±23	103±18	107±19	106±21	105±19	**110±18***	105±15	**98±24***	110±18	N/A	101±25	**106±19***	97±23	**101±22***
Scleral Depth	27±36	**32±27***	39±29	**29±23***	38±28	37±32	32±27	33±28	38±24	**47±35***	37±26	**45±30***	19±23	**27±26***	33±25	31±26
Choroidal Thickness	56 ±13	**46±13***	45±11	**48±11***	54±14	**44±17***	55±11	**48±15***	60±11	**80±20***	70±26	**50±12***	61±14	**56±19***	54±10	**49±15***

EG eye value is significantly different from the contralateral normal eye (Generalized least squares model, $p < 0.005$ due to adjustment for multiple comparisons)*

[1]Included parameters are those with multiple measurements per eye which are required to assess animal-specific EG eye versus Control eye differences

[2]Outer scleral canal and peripapillary scleral parameters are missing for the EG eye of Rat 6 due to poor visualization within its 3D histomorphometric reconstruction.

Supplemental Table 2. Animal Specific Global Values for each Parameter.

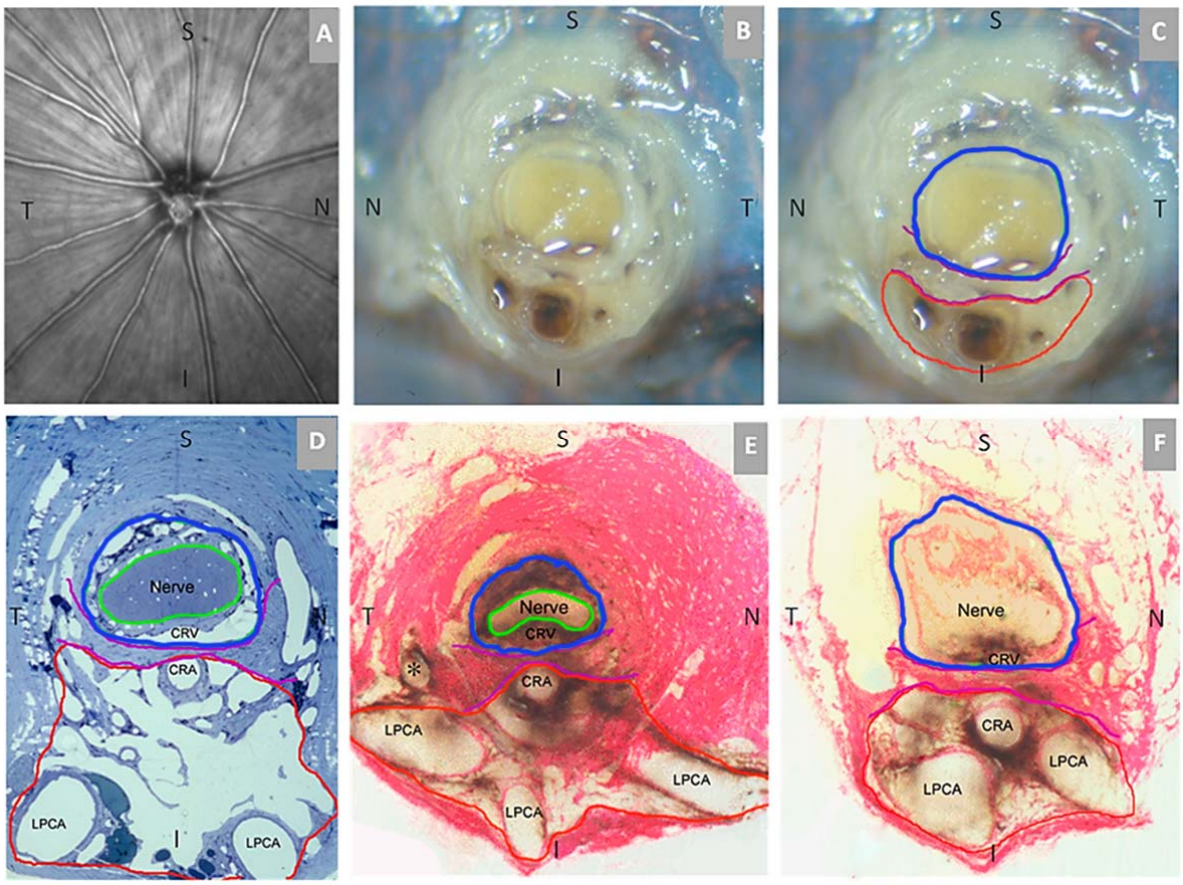

Supplemental Figure 1. Rat Optic Nerve Head Macroscopic and Microscopic Relationships I – Transverse Sections. (A) 30 degree SD-OCT Infrared Reflectance image of the rat optic disc (the vitreal surface of the optic nerve head) (courtesy of Brad Fortune). (B) Macroscopic appearance of the cut surface of the rat optic nerve just posterior to the scleral shell (view from the back of the eye). (C) Principal Macroscopic relationships. The neurovenous bundle (green) and the more-inferior arterial bundle (red) are separated by a sling of scleral tissues (the scleral sling, purple) (view from the back of the eye). (D-E) Principal scleral openings. Unlike the primate, there are two principal openings within the sclera of the rat ONH: 1) the neurovenous canal (blue) and the more-inferior arterial opening (red), which is not a well-defined canal, being irregular due to the choroidal branches of the LPCAs (D and E) and separated from the neurovenous canal by the scleral sling (purple). Unlike the primate, which has on average 15 short posterior ciliary arteries that are evenly distributed around the circumference of the scleral canal, the inferior concentration of the LPCAs and the density of their intrascleral branches to the choroid combined with the actual CRA canal (D – F) suggest an "effective" second opening in the sclera. (D) Transverse histologic section through the scleral portion of the optic nerve head demonstrating the same relationships seen posterior to the globe in panels B and C. Note that the neurovenous bundle consists of the optic nerve surrounded by a vascular tissue within the inferior portion of which runs the CRV. The arterial bundle is made up of the central retinal artery the two main LPCAs and their intrascleral branches to the choroid (vascular spaces in between the principal arteries - not labeled). (E) An acquired, digital transverse section image from a histomorphometric reconstruction demonstrating the same relationships as (D). (F) Digital section image from the same eye just posterior to the globe and close to the view seen macroscopically in (C). The red oblique line in (F) marks the location of a digital radial section image that is not shown. The intrascleral (E) and retrobulbar short posterior ciliary arteries (∗) are branches of the LPCAs rather than the Ophthalmic Artery. A preferential superior-temporal course of the optic nerve and neurovenous bundle as they pass through the sclera into the orbit are suggested by comparing the green circle in (F) to (E). CRV- Central retinal vein, LPCAs- Long Posterior Ciliary Arteries. N – Nasal; T – Temporal; I – Inferior; S – Superior. Reproduced with minor alterations and permission from our previous publication (Pazos et al., 2015).

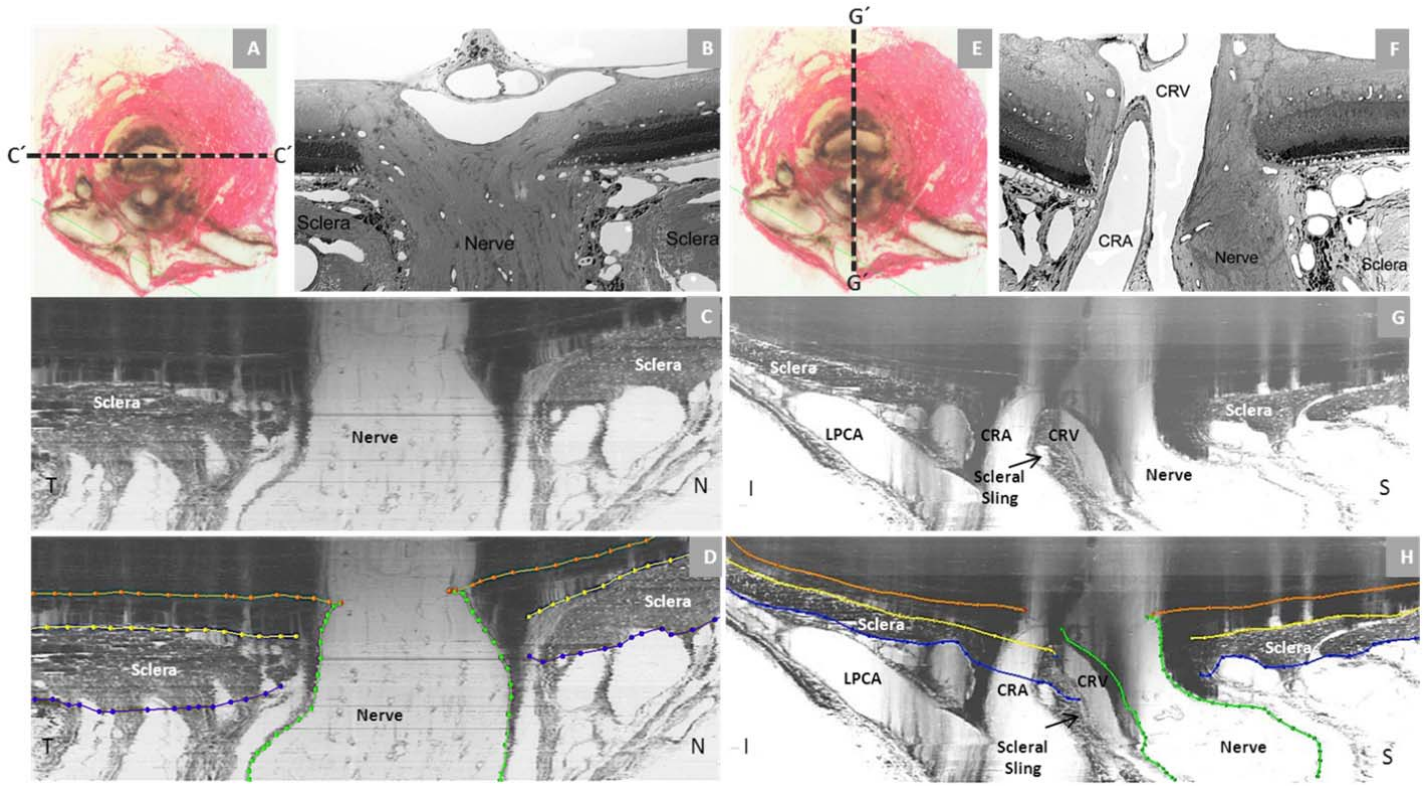

Supplemental Figure 2. Rat Optic Nerve Head Macroscopic and Microscopic Relationships II – Sagittal Sections. Horizontal (upper panels - A, B,C and D) and vertical (lower panels - E, F, G and H) sagittal views of the rat ONH centered upon the scleral portion of the neurovascular canal (A and E). Panels (B, C and D) and (F, G and H) are digital sagittal sections (location relative to the ONH marked as C' and G' in (A) and (E) of the same histomorphometric reconstruction in which acquired transverse section images were shown in Supplemental figure 1 and panels D and H are the same sections showing the delineation of the different structures. The process of creating digital sagittal sections from the histomorphometric volume is explained in Supplemental Figure 3. Panels (B) and (F) are histologic sections of another eye acquired in locations similar to (C) and (G). Most descriptions of the rat ONH show horizontal (C) or vertical (G) sagittal sections of the ONH that are cropped close to the end of the sclera which has the effect of emphasizing the similarities of the neurovenous canal to the scleral canal of the primate. However within the horizontal (C) and vertical (G) digital sagittal sections of the histomorphometric reconstructions, the importance of the venous plexus that surrounds the nerve within the neurovenous canal, the sclera sling and the inferior arterial vessels can be appreciated. Note also the general temporal slant of the nerve in (B) and the superior slant of the nerve in (F). Taken together, these observations within horizontal and vertical sagittal sections confirm the general superior temporal path of the optic nerve tissues suggested within the serial transverse section images of Figure 1 (see Figure legend). Note that within panels (C) and (G) of Figure 2, the dark shadows extending upward from the sclera are a result of the fact that in serial transverse sectioning from the vitreous (top) to the orbital optic nerve (bottom) the dark choroidal pigment can be seen until the sectioning plane passes through it, creating the appearance of a shadow within the retina and vitreous . CRV- Central retinal vein, LPCA- Long Posterior Ciliary Arteries. CRA-Central Retinal Artery; N – Nasal; T – Temporal; I – Inferior; S – Superior. Orange line: Bruch's Membrane, Yellow line: anterior sclera. Blue line: Posterior Sclera. Green line: Nerve boundary. Reproduced with permission from our previous publication (Pazos et al., 2015).

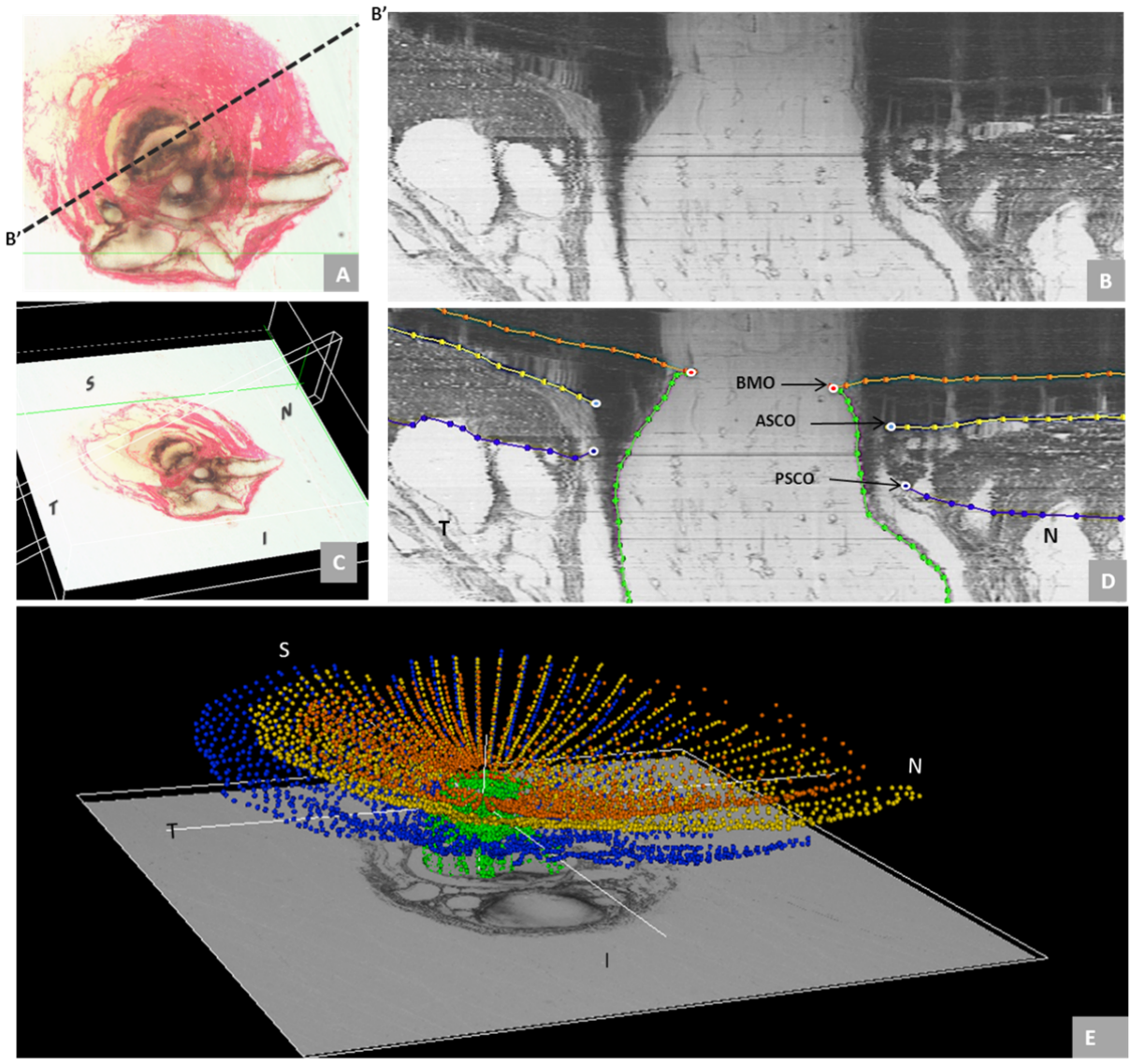

Supplemental Figure 3. Points within 40 Digital Serial Radial Sagittal Section Images of each ONH. The delineator first assigned the center of the scleral portion of the optic nerve (A) to be the center of rotation through which, forty, 7-voxel thick, digital radial sagittal section images (B) of the digital 3-D reconstruction (C) were serially served at 4.5º intervals. The Nasal-Temporal location of (B) is shown here two dimensionally (dotted line marked B-B') within the transverse section image in (A) and three-dimensionally (7 µm thick white-edged rectangle) within the 3-D reconstruction in (C). Within each digital sagittal section image (B) the delineator marked four landmark surfaces and three pairs of neurovenous canal landmarks (one point on each side of the canal). The landmark surfaces were: (1) Bruch's membrane (orange); (2) the anterior (yellow) and (3) posterior (blue) surfaces of peripapillary sclera ; and (4) the optic nerve boundary extending from Bruch's membrane opening, through the scleral canal and along the pia mater to the posterior edge of the reconstruction (green). The landmark points were Bruch's Membrane Opening (BMO – red), the anterior scleral canal opening (ASCO – light blue) and the posterior scleral canal opening (PSCO – purple). A representative point cloud which contains all delineated landmark types for all 40 radial sections of an individual reconstruction is viewed from its superior surface three dimensionally in (D) (temporal is to the left and nasal is to the right). Three dimensional reconstructions of the landmark point clouds (D) of each eye were 3D visualized together and separately (turning each landmark category on and off) so as to qualitatively determine their principal macroscopic relationships. In Panel (E) the superior temporal course of the optic nerve as it passes through the sclera and its sharper bend into the orbit can be appreciated. N – Nasal; T – Temporal; I – Inferior; S – Superior. Reproduced with permission from our previous publication (Pazos et al., 2015).

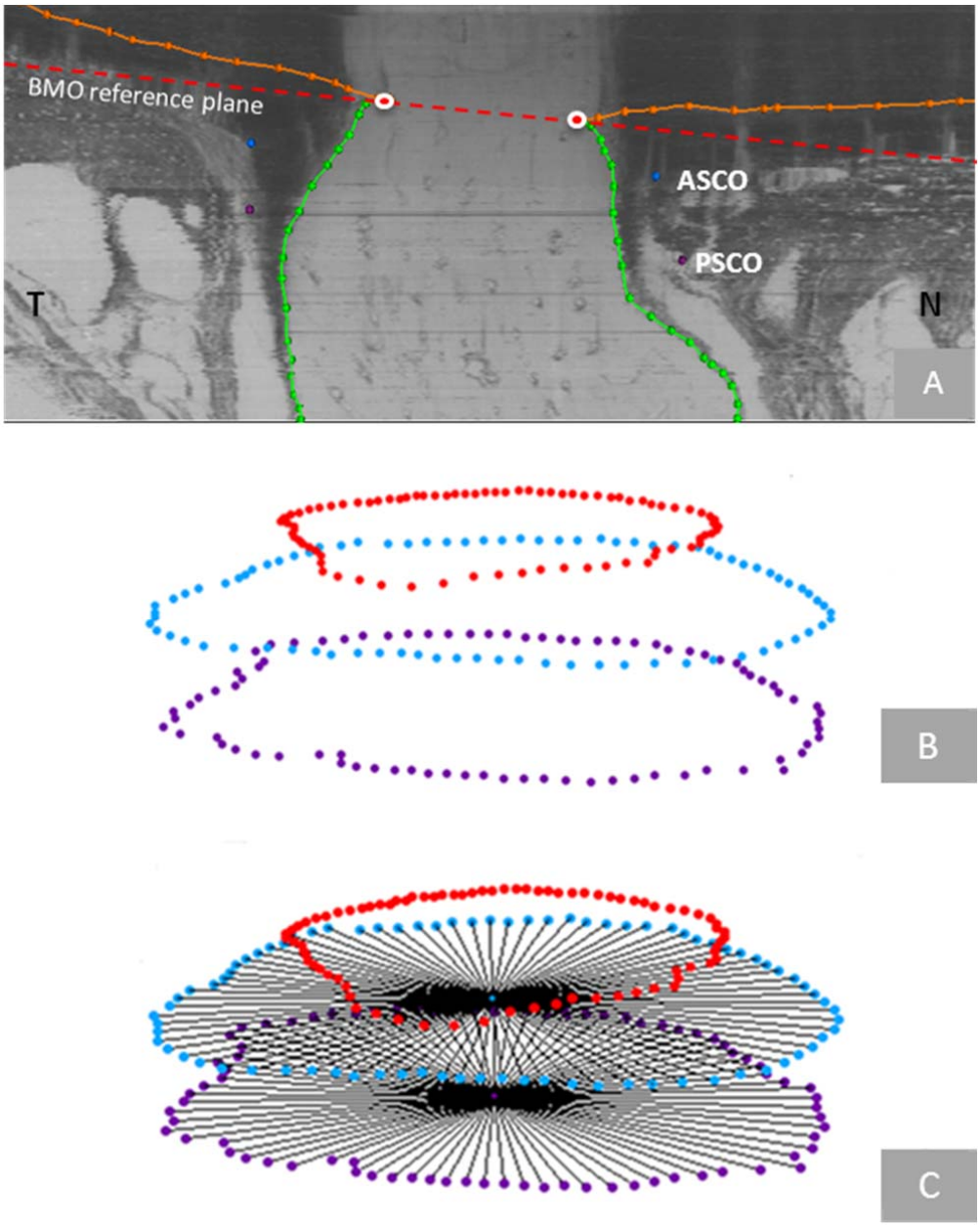

Supplemental Figure 4. Bruch's Membrane Opening (BMO) and Neurovascular Scleral Canal Parameterization. **(A)** Within each ONH reconstruction, individual planes were fit to the 80 BMO points, 80 ASCO points and 80 PSCO points which are illustrated in cross-section within a digital sagittal section image. (**N** – Nasal; **T** – Temporal). **(B)** The cross-sectional area of all three openings (BMO, ASCO and PSCO) was calculated as the area within the projection of the BMO, ASCO and PSCO points to their respective fitted planes. **(C)** Using the centroid of the projected BMO, ASCO and PSCO points, 80 radius measurements were made within their respective fitted planes at 4.5 degree intervals. Reproduced with permission, from Appendix Figure 1 of our previous publication (Pazos et al., 2015).

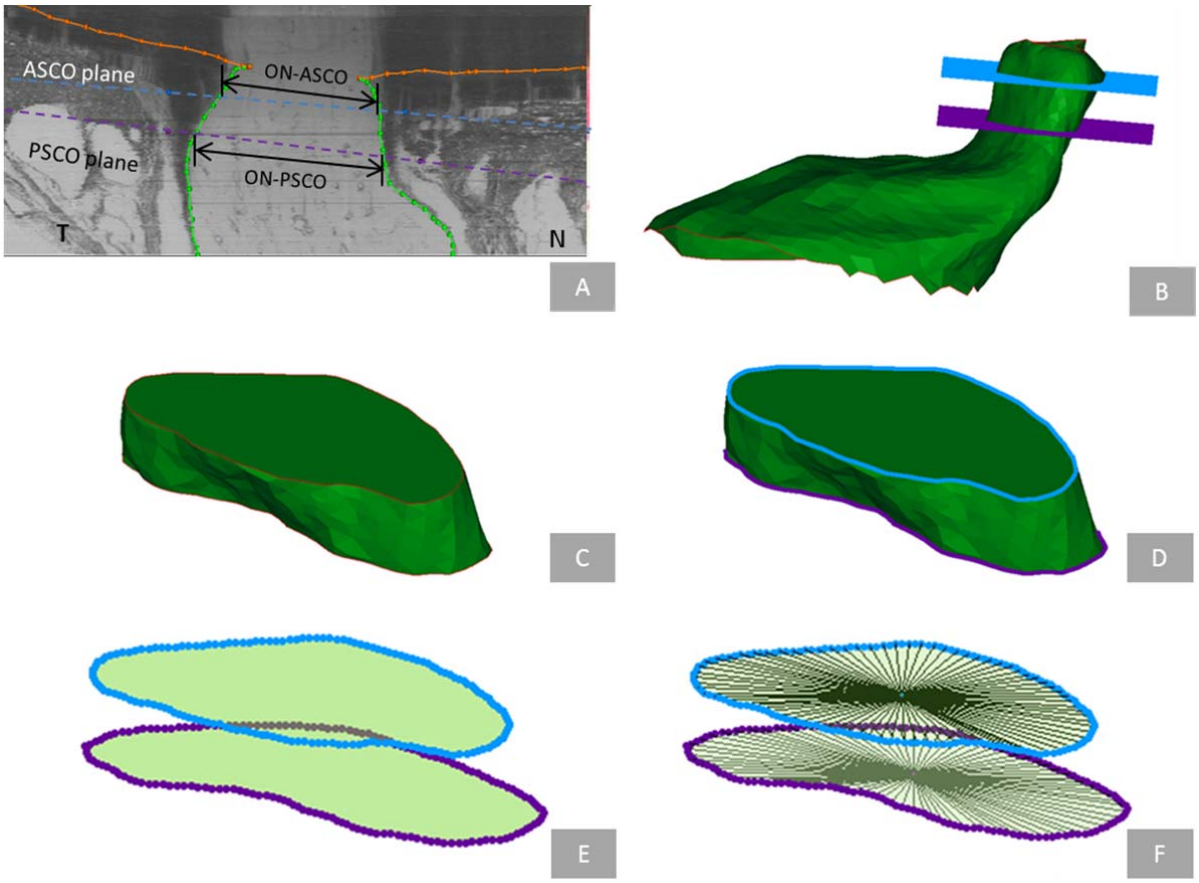

Supplemental Figure 5. Scleral Canal Optic Nerve Area and Volume Parameterization. Optic nerve cross-sectional area and radii were quantified within the ASCO (ON-ASCO) and PSCO (ON-PSCO) planes using the delineated optic nerve boundary (green dots) as illustrated within digital sagittal sections in panel (A). ON cross-sectional area within BMO (ON-BMO) could not be quantified due to obstruction of its boundaries by pigment from the perineural venous plexus. In (B) the optic nerve point cloud (from all 40 delineated sections) has been surfaced (green) and the position of the ASCO (light blue) and PSCO (purple) planes relative to the optic nerve is shown. Please note that while the ASCO and PSCO planes are based on the respective openings within the sclera (Figure 5, above, and panel A of this figure) it is the scleral canal optic nerve volume or the optic nerve volume within the canal (not including the surrounding venous plexus) and between the planes that is isolated within (C). The ON-ASCO (light blue) and ON-PSCO (purple) surfaces of the scleral canal optic nerve volume are highlighted in (D), and their areas and radii are quantified in (E) and (F). The orientation of panels (B) – (F) is approximately that of (A) - Temporal (T) left and Nasal (N) right. Reproduced with permission, from Appendix Figure 2 of our previous publication (Pazos et al., 2015).

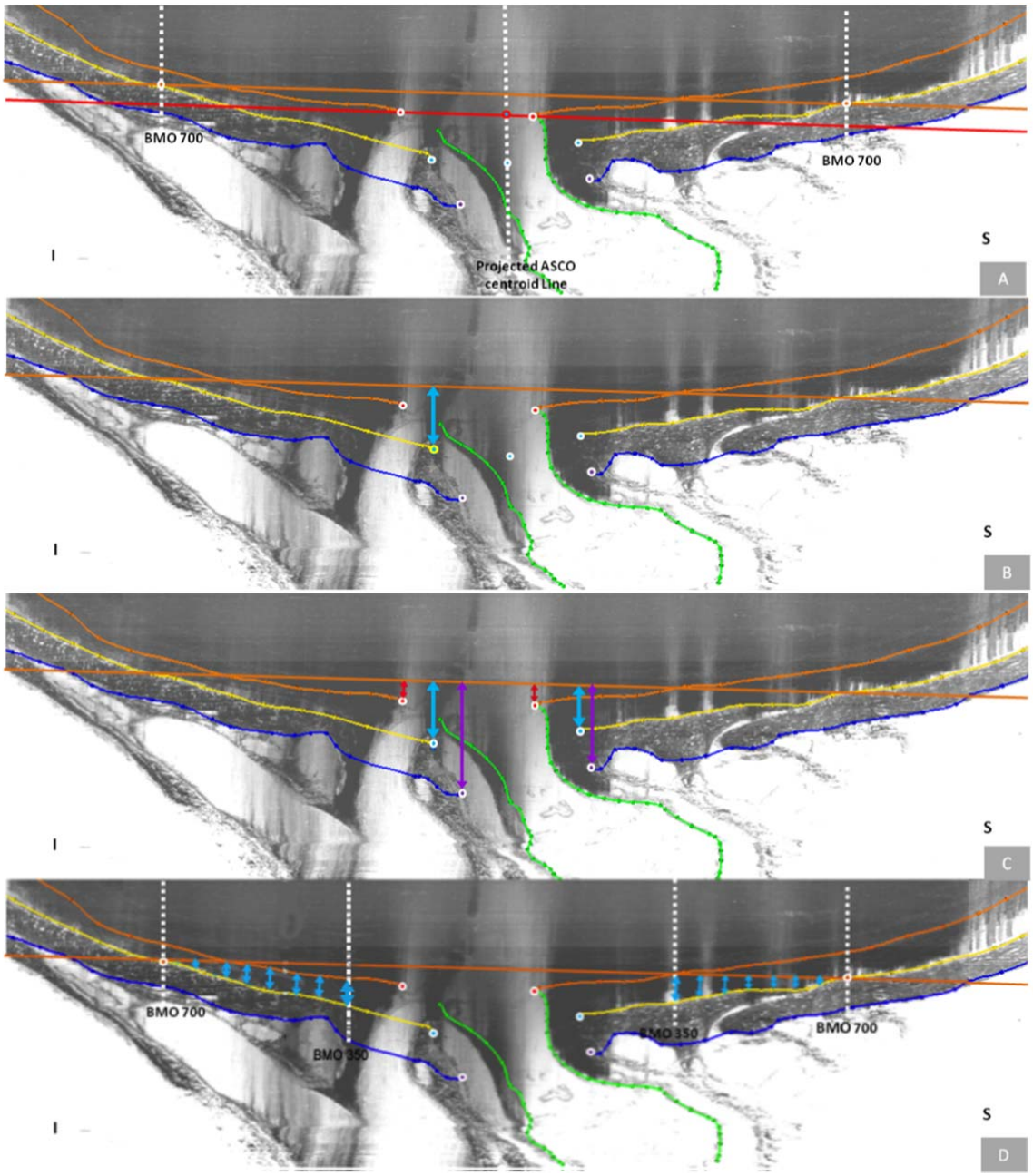

Supplemental Figure 6 *Anterior Scleral Sling Depth*, *BMO Depth* and *Anterior Peripapillary Scleral Depth* relative to a peripheral anterior scleral reference plane. (A) A peripheral anterior scleral reference plane was generated from a ring of points (orange dot with white border) on the anterior scleral surface at a distance 700 microns (BMO 700) from the projected ASCO centroid line. (B) *ASCO Depth (blue arrow)* was measured relative to the peripheral anterior scleral reference plane in each radial section in which the sling surface could be identified (approximately 8 section images per ONH). Circled in yellow you can see the most anterior aspect of the scleral sling. (C) *BMO Depth* was measured for each BMO point relative to the same reference plane within each section. PSCO (purple arrow), ASCO Depth (blue arrow) and BMO depth (red arrow) were calculated relative to this peripheral anterior scleral reference plane as well. (D) *Anterior Peripapillary Scleral Depth* relative to the same reference plane was measured at a distance of BMO 350 to BMO 700 µm (in 50 µm increments) on the fitted anterior scleral surface (yellow line). Red dot with white border – BMO; Blue dot with white border – ASCO; Purple dot with white border – PSCO; Projected ASCO centroid line (A) - perpendicular line to the BMO reference plane (red line) passing through the raw ASCO centroid (blue dot with white border); Blue dot with red border (B) - projected ASCO centroid; *BMO 350/700* - Perpendicular line from the BMO reference plane at a distance of 350/700 µm from the projected ASCO centroid line so as to define BMO 350/700 eccentricity. I – Inferior; S – Superior. . Orange line: Bruch's Membrane, Yellow line: anterior sclera. Blue line: Posterior Sclera. Green line: Nerve boundary. Reproduced with permission, from Appendix Figure 3 of our previous publication (Pazos et al., 2015).

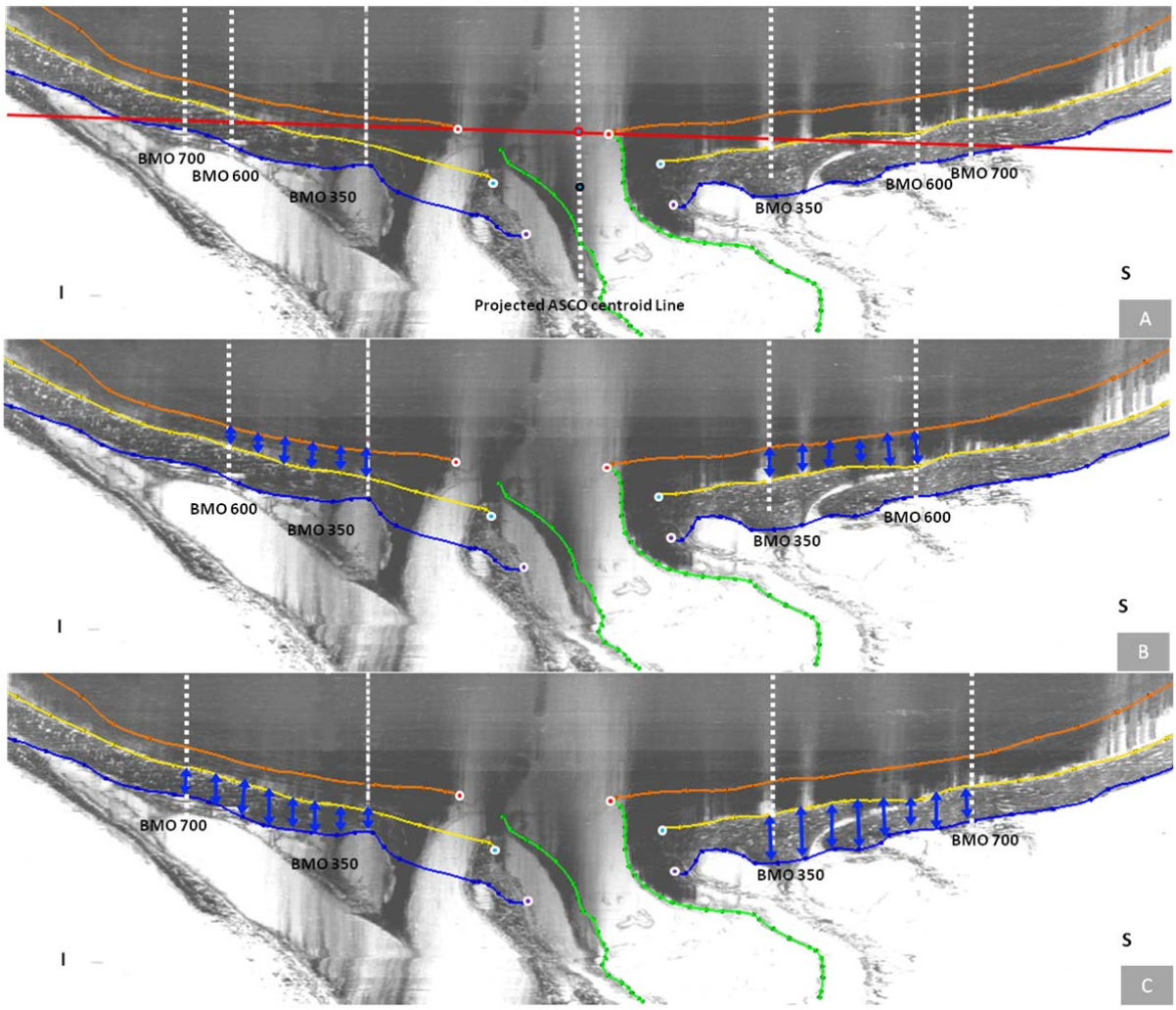

Supplemental Figure 7. *Peripapillary Choroidal* and *Peripapillary Scleral Thickness* Parameterization. (A) Projected ASCO centroid line is a perpendicular line to the BMO reference plane (red line) passing through the raw ASCO centroid (blue dot with black border) and projected ASCO centroid (Blue dot with red border). *BMO 350/600/700*: Perpendicular line from the BMO reference plane at a distance of 350/600/700 □m from the projected ASCO centroid line so as to define BMO 350/600/700 eccentricity. (B) *Peripapillary Choroidal Thickness (dark blue arrows)* was measured perpendicular to Bruch's Membrane surfaces in 50 □m increments along the BMO reference plane between the BMO 350 to BMO 600 landmarks. (C) *Peripapillary Scleral Thickness (dark blue arrows)* was measured perpendicular to the anterior scleral surface in 50 □m increments along the BMO reference plane between the BMO 350 to BMO 700 landmarks Red dots with white border – BMO; Blue dots with white border – ASCO; Purple dot with white border - PSCO. Blue dot with black border (A) – ASCO centroid; I – Inferior; S – Superior. Orange line: Bruch's Membrane, Yellow line: Anterior sclera. Blue line: Posterior Sclera. Green line: Nerve boundary. Reproduced with permission from Appendix Figure 4 of our previous publication (Pazos et al., 2015).

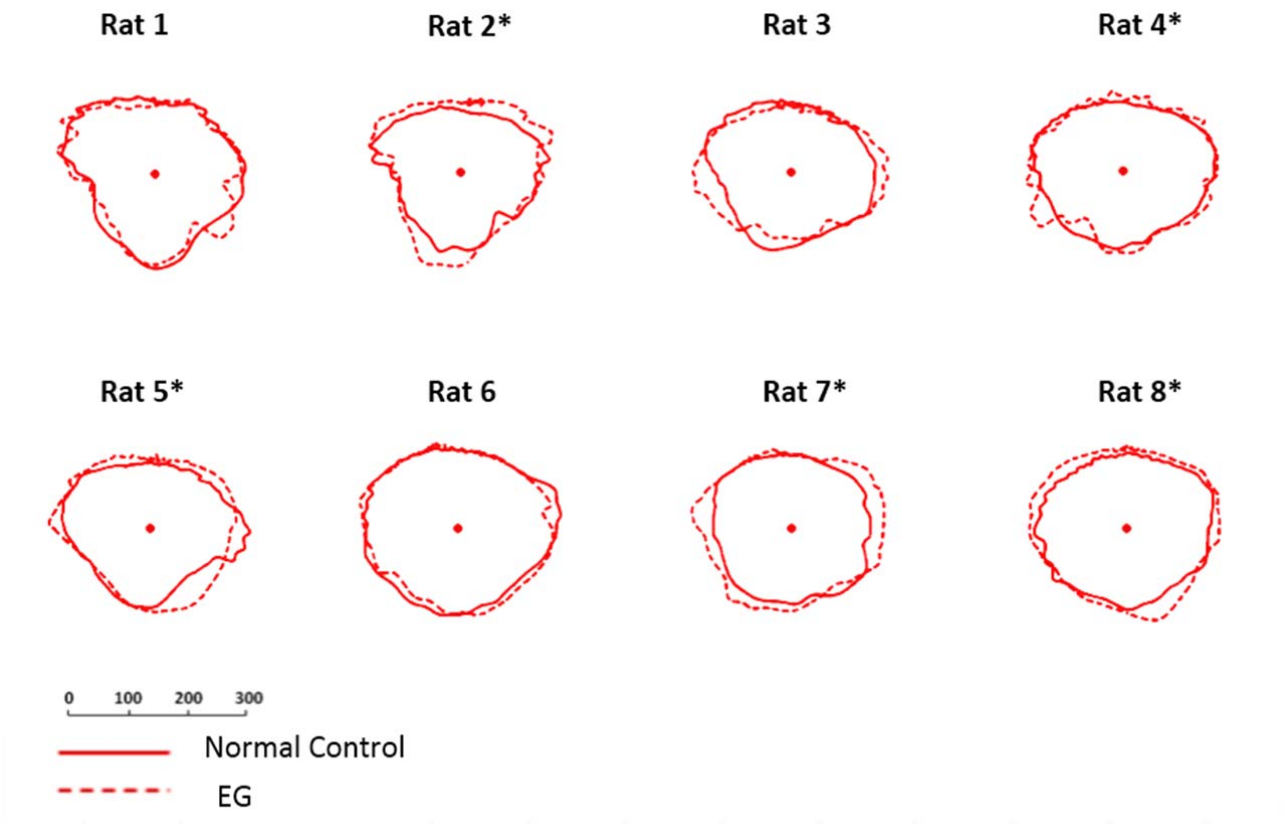

Supplemental Figure 8. EG (dotted line) versus Control (solid line) eye Bruch's Membrane Opening (BMO) comparison for each animal. BMO data points for the Control and EG eye of each rat are schematically overlaid using the BMO centroid of each eye. All data are in right eye orientation. The scale is in micrometers. **(*)** denotes animals in which Global EG versus Control Eye *BMO radius* differences achieved significance (Table 4).

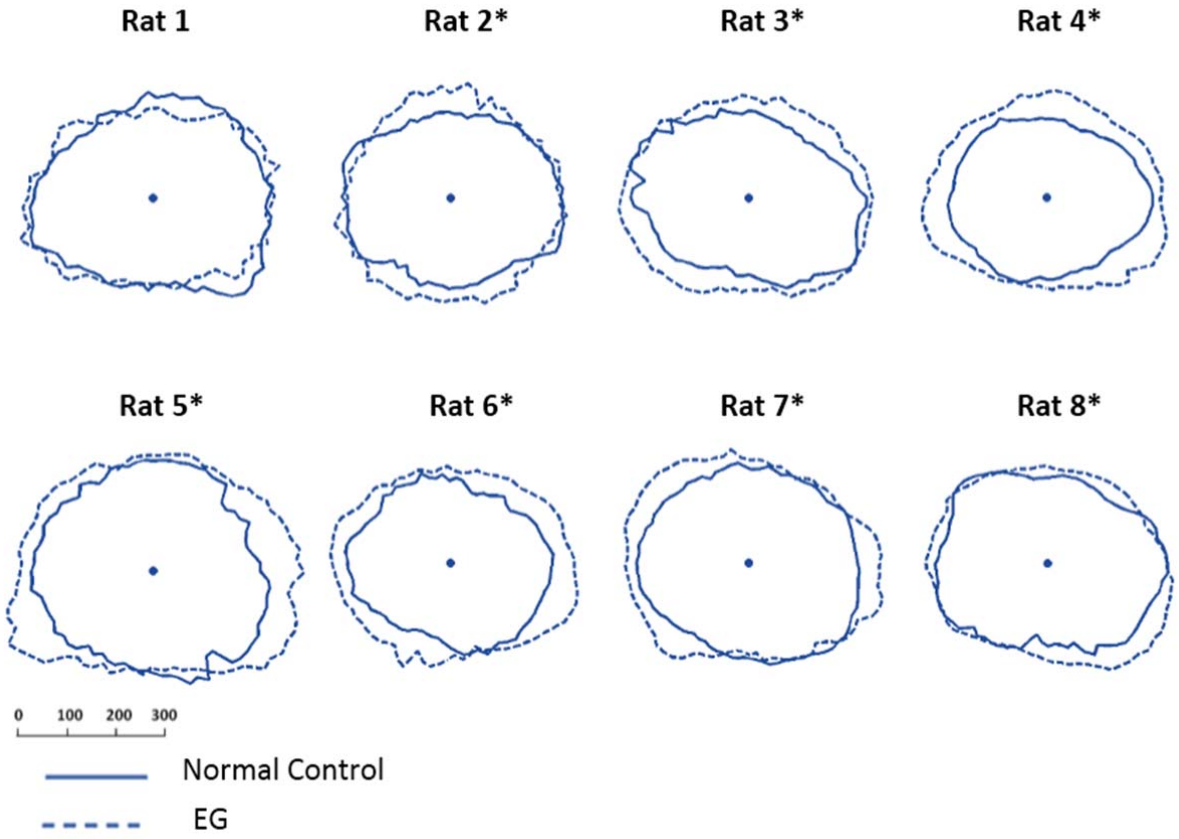

Supplemental Figure 9. EG (dotted line) versus Control (solid line) eye Anterior Scleral Canal Opening (ASCO) comparison for each animal. ASCO data points for the Control and EG eye of each rat are schematically overlaid using the ASCO centroid of each eye. All data are in right eye orientation. The scale is in micrometers. **(*)** denotes animals in which Global EG versus Control Eye *ASCO radius* differences achieved significance (Table 4).

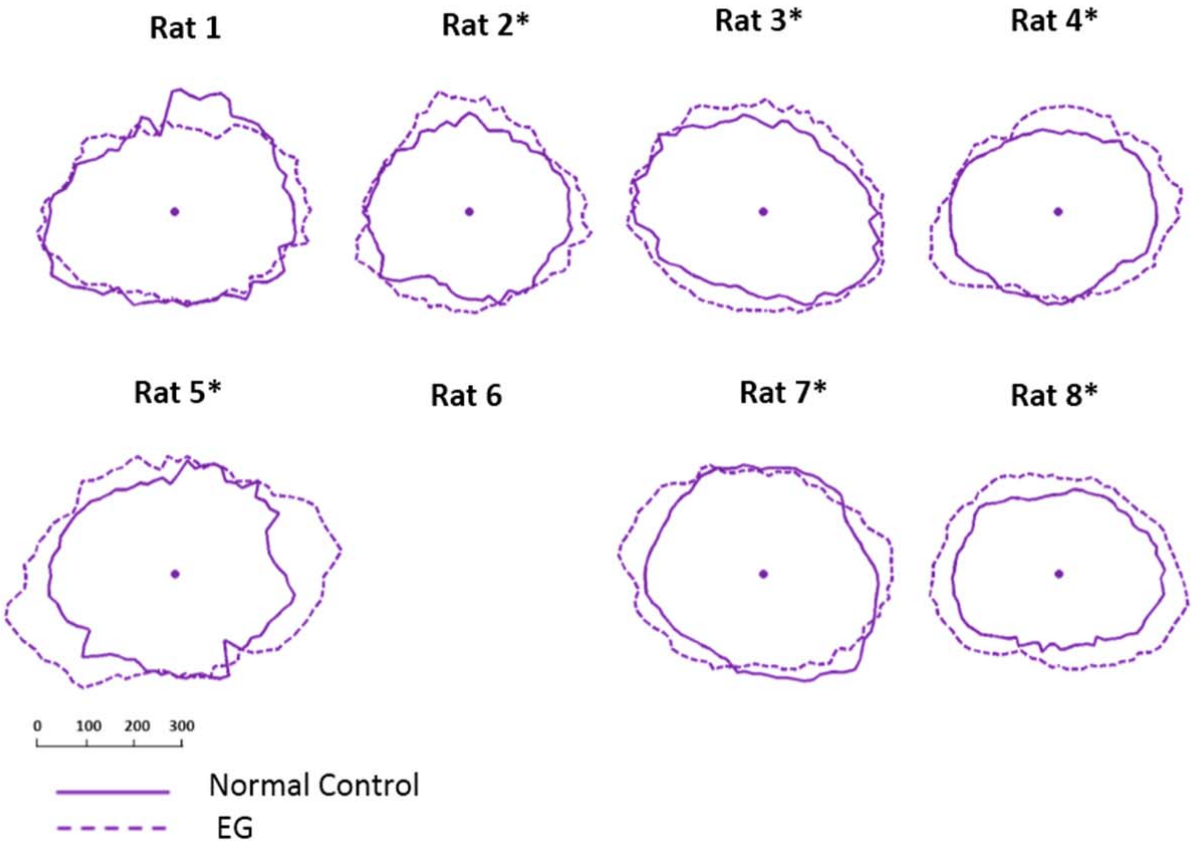

Supplemental Figure 10. EG (dotted line) versus Control (solid line) eye Posterior Scleral Canal Opening (PSCO) comparison for each animal. PSCO data points for the Control and EG eye of each rat are schematically overlaid using the PSCO centroid of each eye. All data are in right eye orientation. The scale is in micrometers. **(*)** denotes animals in which Global EG versus Control Eye P*SCO radius* differences achieved significance (Table 4). PSCO data for the EG eye of Rat 6 were not available.

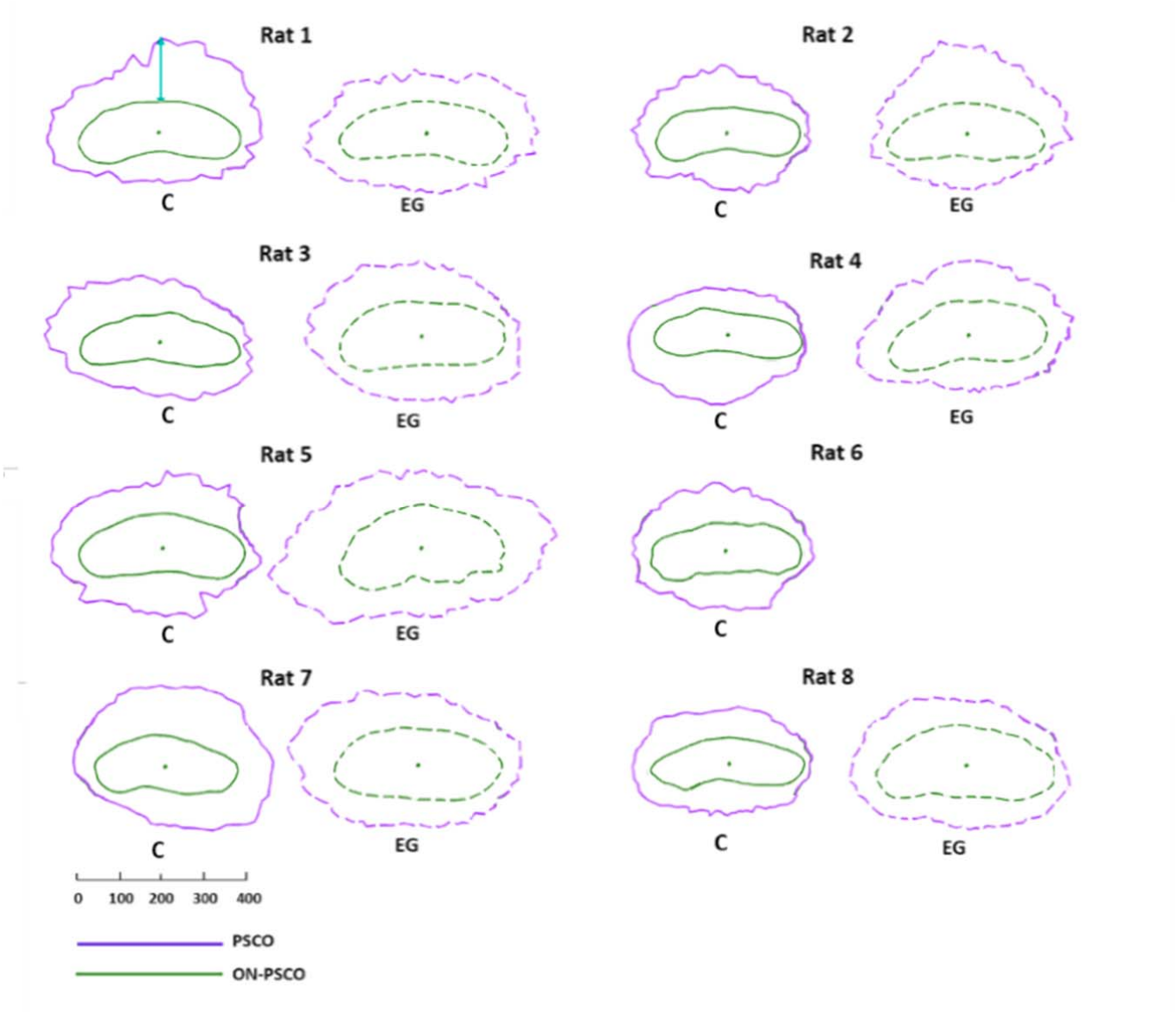

Supplemental Figure 11. Animal-specific, EG (dotted line) versus Control Eye (solid line) comparisons of Posterior Scleral Canal Opening (PSCO – Purple) and Optic Nerve–PSCO (ON-PSCO - green). PSCO fitted spline and ON-PSCO fitted spline are projected onto the PSCO reference plane for comparison purposes. The ON-PSCO centroid for each eye has been used to horizontally align the data from each eye. The green arrow (Control eye of Rat 1, upper left) schematically depicts the *PSCO-ON-PSCO Distance* measurement (here showing 1 of a total of 80 radial measurements – see methods). Animal-specific EG vs Control eye overlays of PSCO and ON-PSCO data can be seen in Supplemental Figures 10 and 12, respectively. Global EG eye *PSCO-ON-PSCO Distance* was significantly increased within Animals 2, 3, 5, and 7. The scale is in micrometers.